한국해양공학회지 제19권 제2호, pp 19~28, 2005 (ISSN 1225-0767)

Responses of Submerged Double Hull Pontoon/Membrane Breakwater

S.T. Kee*
*Dept.of Civil Engineering, Seoul National University of Technology, Seoul, Korea

KEY WORDS: Flexible Membrane, Submerged/Floating Breakwater, Porous Coefficient, Eco-Friendlier Breakwater, Multi-Domains BEM

ABSTRACT: *The present paper outlines the numerical investigation of the incident wave interactions with fully submerged and floating dual double hull pontoon/vertical porous membrane breakwaters. Two dimensional five fluid-domains hydro-elastic formulation was carried out in the context of linear wave body interaction theory to study the wave interaction with the double hull of pontoon-membranes. The submerged circular pontoon is consisted of double hulls, which is filled with water in the void space between the outer structure and inner solid buoyant structure. Hydrodynamic characteristics of the proposed system with dual floating double-hull-pontoons filled with water have been studied numerically for the various incident waves. This study is a beginning stage research for the dual double hull porous pontoons/vertical porous membranes breakwaters which is ideally designed in order to suppress significantly the transmitted and reflected waves simultaneously.*

1. INTRODUCTION

The desirable characteristics of floating flexible membrane systems include their reduced environmental impacts, ability of relocation/rapid-deployment, simple sacrificial or reusable design, and comparably low cost in constructions. Thus, it can be used for a portable temporary breakwater to protect various coastal or offshore structures, and sea operations requiring relatively calm sea states. In view of this, a number of vertical floating flexible membrane breakwaters have been investigated by Thompson et al. (1992), Aoki et al. (1994), Kim and Kee (1996), Williams (1996), Kee and Kim (1997), Cho et al. (1997, 1998), Edmond (1998), Kee (2001a, b), Lee and Edmond (2002), and Kee et al. (2003).

Kim and Kee (1996) developed an analytical model for wave transmission and reflection by a vertical pre-tensioned membrane using the eigenfunction expansion method and presented a numerical solution of the problem employing simple source distribution method. Kee and Kim (1997) have developed a theory and a numerical solution for a surface piercing or fully submerged and mechanically coupled system. These methods were applied to vertical floating flexible membrane systems in oblique seas by Cho et al. (1997). Cho et al. (1998) partially extended the work by Kee and Kim (1997) and developed a boundary integral method solution for dual buoy-membrane system with either a surface piercing or fully submerged buoy in oblique seas. Kee (2001a, b) investigated the performances of the fully submerged and floating double buoy/porous membrane breakwaters that are hinged at some distances over sea bottom and placed in parallel with spacing needs to be evaluated for arbitrary incident wave angles and for various permeability on membranes.

The proposed system, called as an eco-friendlier breakwater, can insure marine scenario, sediment transport, fish passage, surface vessel passing, the water circulation to prevent stagnation and pollution in the sheltered region, and the reduced hydrodynamic pressures on the body of structures. Lee and Edmond (2002) investigated the performance of surface penetrating flexible single or dual membrane wave barriers of finite draft. The dual system was found to be highly efficient, compared to the single system in the low frequency range, mainly due to the wave trapping effects. The system was, however, lack of the practical engineering consideration, since the taught pretension of membranes was assumed to be provided externally.

Kee et al. (2003) studied the mechanism of wave blocking, dissipating, and partial trapping effects of the proposed system by Kee (2001a, b). It was found that the fully submerged floating double buoy/porous membrane breakwaters acts as a wave scatterer reducing the incident wave amplitude by the mutual cancelation based on the phase differences between incident and scattered waves, dissipating wave energy through fine pores on membranes, partially trapping the incident waves, and even re-reflecting between the two systems. The wave blocking efficiency of the proposed breakwater was found to be very high along the wide range of frequency and wave headings. In the high frequency ranges, however, the reflected waves were relatively high, since the wave energy dissipation hardly obtained through the deep submerged pores on the membranes.

제1저자 기성태 연락처: 서울시 노원구 공릉2동 172
02-970-6509 stkee@snut.ac.kr

Ideally, the breakwater should, as we expect intuitively, have the minimum transmission at lee side. It is also often desirable that the reflection should be small for the protection of the vessel passing over or at the front of system. In order to suppress significantly the reflected waves in the region of high frequency, it is necessary for the proposed system to have the permeability on the surface of the fully submerged buoy, obtaining the further wave energy dissipation based on the fluid viscosity at the near of free water surface.

In this point of view, the performance of the fully submerged floating double hull pontoon/porous membrane breakwaters as shown in Fig. 1 was investigated, in the present study, as a beginning stage of research for the final target; the porous double hull pontoon/porous membrane breakwaters. It is assumed, for simplicity, that the heave motion of the rigid and large pontoon is negligible due to the large initial tension by its buoyancy. When the size of the pontoon is not small, we have to solve the diffraction and radiation of the pontoon, and its dynamic interaction with membrane in addition to the wave membrane interaction. The velocity potentials of wave motion are fully coupled with membrane deformation. The static tension by the buoyancy is much greater than the dynamic tension, thus the initial tension of membrane is assumed to be constant. This problem is solved by the distribution of the simple sources (modified Bessel function of the second kind) that satisfy the Helmholtz governing equation in three fluid domains.

The accuracy and convergence of the developed multi-domains BEM code were checked based on the energy conservation formula for a limited case. The hydrodynamic characteristics of the double hull system has been studied for the various inner pontoon radiuses against its outer radius, which are slightly modified using the optimally tuned single hull system. The single hull optimum system was chosen in the previous studies (Kee et al., 2003), through a series of the parametric investigations with various parameters of drafts, membrane lengths, clearances, gaps, spacing, mooring lines stiffness, mooring types, and water depth. It was found that the dual floating double hulled pontoon (filled with water)/ membrane breakwaters can, if it is properly tuned for mutual cancellation to the coming waves, have better performances in transmitting the incident waves over a mid range of wave frequency than that of single hull pontoon. It is also found that the exciting forces inside of the double hull by the disturbed complex velocity potential are directly related to the motion of pontoon with membrane which interacts with incident waves.

2. THEORY AND NUMERICAL METHOD

So we consider the interaction of the dual floating pontoon/membrane wave barrier with obliquely incident waves. As shown in Fig. 1, the submerged dual system is composed of fully submerged double hull pontoon/vertical flexible porous membrane placed in parallel with spacing, and allows the flow passing over and beneath structures.

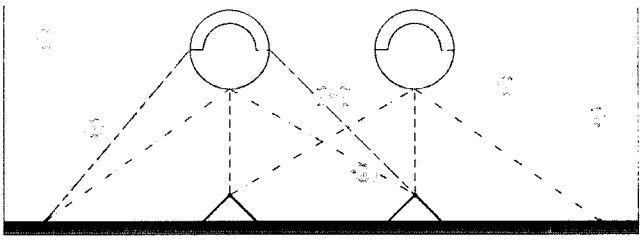

Fig. 1 Conceptual sketch

An inertial, Cartesian coordinate system (x, y) with its origin, located at the still water level, is used as reference system. In Fig. 2, the front submerged breakwater is placed at $x=0$. and the rear breakwater is installed at $x=d_c$ The pontoon/membrane system allows gaps c_{ik} for $i=f, r;\ k=f, b$ for example $c_{ff}, c_{fb}, c_{rf}, c_{rb}$ which present a front free surface gap, a front bottom gap, a rear free surface gap, and a rear bottom gap, respectively.

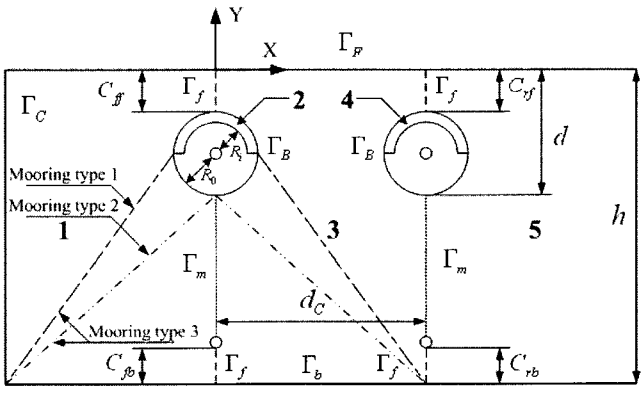

Fig. 2 Coordinate system and integration domains.

The system is idealized as two dimensional problem allowing that wave and system motions are uniform in Z direction. The integration fluid domain is subdivided into

five domains. A plane monochromatic incident wave train with small amplitude A and harmonic motion of frequency ω propagates towards the breakwater with an angle θ (wave heading) with respect to x axis in water of constant depth h The ideal flow field can be described in terms of the time harmonic total velocity potential for an oblique incident wave:

$$\Phi(x,y,z,t)=Re[\{\phi_0(x,y)+\phi(x,y)\}e^{ik_z z-i\omega t}] \quad (1)$$

where Re denotes the real part of a complex expression, $i=\sqrt{-1}$, t denotes time, and $k_z=k_0\sin\theta$ is the wave number component in the z direction, and k_0 is the wave number of the incident wave, which is the positive real solution of the dispersion equation $\omega^2=k_0 g\tanh k_0 h$ with g being the gravitational coefficient. Then, the velocity potential of small amplitude of wave train hight A wavenumber k_0, and wave heading θ is given by

$$\phi_0=\frac{igA}{\omega}\frac{\cosh k_0(y+h)}{\cosh k_0 h}e^{ik_0\cos\theta x} \quad (2)$$

where, ϕ_0 is the known incident potential, and ϕ is the time independent unknown scattered potential, which includes both diffraction and radiation effects. The unknown scattered complex velocity potentials, ϕ_l in five fluid domains $l=1,2,3,4,5$ (Fig. 2), satisfy the Helmholtz equation as a governing equation and the following linearized free surface (Γ_F), bottom (Γ_b), and Sommerfeld radiation conditions (Γ_C):

$$\nabla^2\phi_l-k_z^2\phi_l=0 \qquad (l=1,2,3,4,5) \quad (3)$$

$$-\omega^2\phi_l+g\frac{\partial\phi_l}{\partial y}=0 \qquad \text{on } \Gamma_F \quad (4)$$

$$\frac{\partial\phi_l}{\partial n}=0 \qquad \text{on } \Gamma_b \quad (5)$$

$$\lim_{x\to\infty}\left(\frac{\partial}{\partial x}\pm ik_x\right)(\phi_l)=0 \quad \text{on } \Gamma_C,\ l=1,5 \quad (6)$$

where Γ_C is the vertical truncation boundaries at far fields and $\mathbf{n}=(n_x,n_y)$ is the unit outward normal vector. In the numerical implementation, the radiation boundary condition is applied on Γ_C located at a finite distance (3~4 times of the water depth) from the edge of structure. In addition, the surface and bottom gaps between fluid domains must satisfy the following vertical fictitious (matching) boundary condition (Γ_f) based on the continuity of hydrodynamic pressure and normal fluid velocity:

$$\phi_l=\phi_{l+1},\ \frac{\partial\phi_l}{\partial x}=-\frac{\partial\phi_{l+1}}{\partial x} \qquad \text{at } \Gamma_f \quad (7)$$

Based on Darcy's law, the normal velocity inside of membrane with fine pores is linearly proportional to the pressure difference between the two sides of the membrane (Wang and Ren, 1993):

$$W(y,t)=\frac{b}{\mu}(p_1-p_2)=\frac{b}{\mu}\rho i\omega(\phi_l-\phi_{l+1})e^{-i\omega t} \qquad \text{at } x=0,d_c \quad (8)$$

The scattered complex unknown velocity potentials must satisfy the following linearized kinematic boundary conditions on the porous-membrane surface:

$$\frac{\partial\phi_l}{\partial x}=-\frac{\partial\phi_{l+1}}{\partial x}=-i\omega\xi+\frac{b}{\mu}\rho i\omega(\phi_l-\phi_{l+1}) \quad (9)$$

where μ is constant coefficient of dynamic viscosity, ρ is constant fluid density, and b is a material constant called permeability having the dimension of a length, and the harmonic membrane motions $\Xi(y,t)=Re[\xi(y)e^{ik_z z-i\omega t}]$. For simplicity, the heave motion of the pontoon is assumed negligible under large initial tension of membrane. Then the boundary condition on the floating pontoon is

$$\frac{\partial\phi_l}{\partial n}+i\omega(\eta_1 n_x+\eta_3 n_\theta)+\frac{\partial\phi_0}{\partial n}=0 \text{ on } \Gamma_B \quad (10)$$

where $n_\theta=xn_y-yn_x$, and the symbols η_1,η_3 represent complex sway and roll responses of pontoons, respectively. Since circular pontoons are connected to the membranes, the coupled dynamic equations need to be solved. Unlike rigid body hydrodynamics, the body boundary condition on membrane is not known in advance. Therefore, the membrane and pontoon motions and velocity potentials need to be solved simultaneously.

To solve the present boundary value problem, a five domain boundary integral equation method using simple sources along the entire boundary is developed. Using Green's second identity, the unknown scattered potential can be expressed as

$$C\phi_l(x,y)=\int_\Gamma\left\{\phi_l(x',y')\frac{\partial G}{\partial n}-G(x,y,x',y')\frac{\partial\phi_l}{\partial n}\right\}d\Gamma \quad (11)$$

where C = solid angle constant and the integral covers the entire boundary of each fluid region, (x, y) and (x', y') are field point and source point, respectively. The fundamental solution (Green function) of the Helmholtz equation and the normal derivative of G are given by:

$$G=-\frac{1}{2\pi}K_0(k_z r),\ \frac{\partial G}{\partial n}=\frac{1}{2\pi}k_z K_1(k_z r)\frac{\partial r}{\partial n} \quad (12)$$

When the source point shrinks to the field point on boundary i.e., when $r\to 0$ a singularity exists due to the presence of $K_0(k_z r)$, and the analytic solution for this integration is impossible. One can use the following existing approximations in the Cauchy principal value sense.

$$\int_\Gamma \lambda K_1(k_z r)\frac{\partial r}{\partial n}d\Gamma=0,$$
$$\int_\Gamma K_0(k_z r)d\Gamma=\int_\Gamma -r-\ln\left(\frac{k_z r}{2}\right)d\Gamma \quad (13)$$

Applying Green's second identity in each of the domains to the unknown potentials ϕ_l and imposing the relevant boundary conditions eqs. (3)~(10), the integral equations in fluid domain 1, 2 can be written as

$$C\phi_1+\int_{\Gamma_F}\left\{k_z K_1(k_z r)\frac{\partial r}{\partial n}-\nu K_0(k_z r)\right\}\phi_1 d\Gamma+$$
$$\int_{\Gamma_C}\left\{k_z K_1(k_z r)\frac{\partial r}{\partial n}-ik_x K_0(k_z r)\right\}\phi_1 d\Gamma+$$
$$\int_{\Gamma_{Bw}}\phi_1 k_z K_1(k_z r)\frac{\partial r}{\partial n}+K_0(k_z r)\frac{\partial \phi_0}{\partial n}d\Gamma+$$
$$\int_{\Gamma_B}K_0(k_z r)i\omega(\eta_{1f}n_x+\eta_{3f}n_\theta)d\Gamma+$$
$$\int_{\Gamma_{Bb}}\phi_1\left\{k_z K_1(k_z r)\frac{\partial r}{\partial n}-i\rho\omega\frac{b_{Bf}}{\mu}K_0(k_z r)\right\}+$$
$$\phi_2 i\rho\omega\frac{b_{Bf}}{\mu}K_0(k_z r)+K_0(k_z r)\frac{\partial \phi_0}{\partial n}d\Gamma+$$
$$\int_{\Gamma_m}[\phi_1\left\{k_2 K_1(k_z r)\frac{\partial r}{\partial n}-i\rho\omega\frac{b_{mf}}{\mu}K_0(k_z r)\right\}+$$
$$\frac{b_{mf}}{\mu}i\rho\omega K_0(k_z r)\phi_3+(i\omega\xi_f)K_0(k_z r)+$$
$$K_0(k_z r)\frac{\partial \phi_0}{\partial n}]d\Gamma+$$
$$\int_{\Gamma_b}\phi_1 k_z K_1(k_z r)\frac{\partial r}{\partial n}d\Gamma=0 \quad (14a)$$

$$C\phi_2+\int_{\Gamma_B}\phi_2 k_z K_1(k_z r)\frac{\partial r}{\partial n}+K_0(k_z r)\frac{\partial \phi_0}{\partial n}d\Gamma+$$
$$\int_{\Gamma_B}K_0(k_z r)i\omega(\eta_{1f}n_x+\eta_{3f}n_\theta)d\Gamma+$$
$$\int_{\Gamma_B}\phi_2\left\{k_z K_1(k_z r)\frac{\partial r}{\partial n}-i\rho\omega\frac{b_{Bf}}{\mu}K_0(k_z r)\right\}+$$
$$\phi_1 i\rho\omega\frac{b_{Bf}}{\mu}K_0(k_z r)+\phi_0 i\rho\omega\frac{b_{Bf}}{\mu}K_0(k_z r)d\Gamma+$$
$$\int_{\Gamma_B}\phi_2\left\{k_z K_1(k_z r)\frac{\partial r}{\partial n}-i\rho\omega\frac{b_{Bf}}{\mu}K_0(k_z r)\right\}+$$
$$\phi_3 i\rho\omega\frac{b_{Bf}}{\mu}K_0(k_z r)+\phi_0 i\rho\omega\frac{b_{bi}}{\mu}K_0(k_z r)d\Gamma=0 \quad (14b)$$

where $\nu=\omega^2/g$ is the infinite depth wave number, fluid domain 1 and 2 have three interface boundaries between fluid domains 1, 2, and 3. Each integral equations in fluid domain 3, 4, 5 can be formulated based on same approach with the count clockwise integration for outward normal direction in each fluid domain.

In eqs. (14a,b), all the boundary conditions of ϕ_l except for the dynamic boundary conditions of pontoon and membrane can be straightforwardly implemented. In fluid domain 3, geometries of half front pontoon and half rear pontoon exist. In addition, backward side of front membrane and forward side of rear membrane is coexisting with spacing d_c. The integral Eqs. (14a, b) and the other three integrations expanded to the fluid region 3, 4, 5 should be coupled with the equations of motion of the membranes (ξ) and pontoons (η_1 and η_3). In addition, the disturbance potentials must satisfy the following linearized dynamic boundary conditions on the membrane surface:

$$\frac{d^2\xi}{dy^2}+\lambda^2\xi=-\frac{\rho i\omega}{T}(\phi_l-\phi_{l+1})\ on\ \Gamma_m \quad (15)$$

where $\lambda=\omega\sqrt{m/T}$ with T and m being the membrane tension and mass per unit length, respectively. For a numerical approach the discrete form of the equation of membrane motion for $j-th$ element is given by:

$$\rho i\omega(\phi_{l(j)}-\phi_{l+1(j)})l_j-T_{(j)}\left(\frac{\partial\xi}{\partial\zeta}\right)_j+T_{(j+1)}\left(\frac{\partial\xi}{\partial\zeta}\right)_{(j+1)}$$
$$=-ml_j\omega^2\xi_{(j)} \quad (16)$$

where $(\partial\xi/\partial\zeta)_j=(\xi_{(j)}-\xi_{(j-1)})/\triangle\zeta_j$, l_j is the length of the $j-th$ segment, and $\triangle\zeta_j=(l_j+l_{(j+1)})/2$. The geometric boundary conditions at the seabed and the top connection points of membrane $(0,-r_c)$ are $\xi=0$ at $y=-h$, and $\xi=\eta_1+R\eta_3$ at $y=-r_c$. R is distance from the connection point $(0,-r_c)$ to rotation center of a pontoon.

Next, we consider the rigid body motion of the double hull circular pontoon, which is filled with water in the space of the outer hull. As mentioned before, it is assumed that the heave response is negligible due to large initial tension supplied by it huge buoyancy force. The coupled equations of motion for sway and roll are given by

$$M(-\omega^2)X=F_p-(K_{HS}+K_m)X-F_T+F_D \tag{17}$$

where X is displacement of sway and roll, M is a mass matrix of double hull pontoon filled with water, F_p is hydrodynamic forces and moments on a pontoon placed in front side, which includes the exciting velocity complex potentials in the exterior and interior of the double hull, can be written as follows

$$F_p=i\rho g a\begin{Bmatrix} \sum_{outside}(\phi_1+\phi_0)n_x\triangle l_j+(\phi_3+\phi_0)n_x\triangle l_j+\sum_{inside}\phi_2 n_x\triangle l_j \\ \sum_{outside}(\phi_1+\phi_0)n_y\triangle l_j+(\phi_3+\phi_0)n_y\triangle l_j+\sum_{inside}\phi_2 n_y\triangle l_j \\ \sum_{outside}(\phi_1+\phi_0)n_\theta\triangle l_j+(\phi_3+\phi_0)n_\theta\triangle l_j+\sum_{inside}\phi_2 n_\theta\triangle l_j \end{Bmatrix} \tag{18}$$

K_{HS} is the restoring forces and moments due to the hydrostatic pressure, K_m is sway and roll mooring stiffness coefficients including the effects of pretension for the comparison with experimental results (here, pretension is not given for the numerical calculations only), F_D is the nonlinear viscous drag force, and F_T is forces and moments on the pontoons caused by the initial tension of membrane at the connection points between membranes and pontoons, and these are detailed in Kee and Kim (1997).

The obtained integral Eqs. (14a, b) for scattered potentials ϕ_l for two fluid domains can be easily expended to the whole five fluid domains (l=1,2,3,4,5). So far, we obtain the integral equation for five fluid domain (not described here), an equation (16) of membrane motions, and an equation (17) of circular pontoon motions. Those equations are mutually coupled, so they need to be solved simultaneously. If we discretize fluid domain 1 and 5 by $NE_{1,5}$ segments, and discretize interior domain in front and rear pontoons 2, 4 by NE_2, NE_4, respectively, and a middle domain 3 by NE_3, we have $2NE_{1,5}+NE_2+NE_4$ unknowns for the scattered velocity potentials ϕ_1, ϕ_2, ϕ_3, ϕ_4, ϕ_5 and $N_{mf}+N_{mr}$ unknowns for displacement of membranes (ξ_f, ξ_r), and four more unknowns motions of pontoons (η_A, η_B) and (η_A, η_B) where the subscripts (f, r) mean front and rear, respectively. Therefore, we have to solve NT number of linear simultaneous equations. Here the numbers of $NE_{1,5}$, NE_3, NE_2, NT are given by

$$\begin{aligned} NE_{1,5}&=N_F+N_C+N_b+N_{mf}+N_{mr}+N_{Bf}+N_{Br} \\ NE_3&=N_F+N_b+N_{mf}+N_{mr}+N_{Bf}+N_{Br} \\ NT&=2N_{1,5}+N_2+N_4+N_3+N_{mf}+N_{mr}+4 \end{aligned}$$

where, NE_2 , NE_4 are the number of elements of inside of the double hull fluid domain.

3. NUMERICAL RESULTS AND DISCUSSIONS

The five fluid domains boundary element program has been developed based on the linear potential theory and Darcy's law as described in the preceding section, and was used to demonstrate the performance of fully submerged dual pontoon/membrane floating breakwaters in oblique seas. Based on the previous study (Kee et al., 2003), the best performance can be achieved for the dual moorings (type 3) for the front system and the single mooring (type 2) for the rear system with relatively taught mooring stiffness. The toe angles of mooring type 1 and 2 are set as 33° and 29.6°, respectively (Fig. 2).

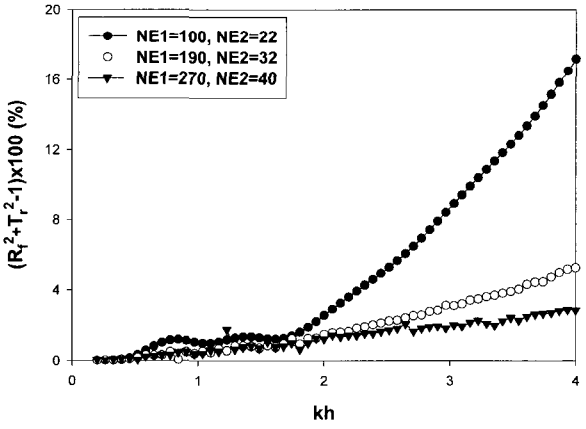

Fig. 3 Convergence test of the developed BEM

The convergence of the developed BEM program for the gradual increments of the number of elements on the whole fluid boundaries is shown for a monochromatic incident wave and the system design parameter of T_i/K_{ij}=0.1 , t_i/R_0=0.02 (dimensionless thickness of pontoon), R_0/h=0.2, R_i/h=0, c_{ik}/h=0.125, d_c/h=1, b=0 (no permeability on membrane). If there is no wave energy dissipation, the energy relation $R_f^2+T_r^2$=1

must be satisfied. The error of deviation, as percentages, from the energy relation are shown in Fig. 3. The symbols R_f, T_r notate reflection and transmission coefficients, respectively. The symbol $T_i\,(i=f,r)$ notate the tension of front (f) and rear (r) membranes, and $K_{ij}\,(i=f,r;\,j=1,2)$ notate mooring stiffness. Here $j=1,2$ denotes upper ($j=1$) and lower ($j=2$) mooring lines. Using $NE_1=270$, $NE_2=40$, the maximum error can be limited under 3% in the entire frequency ranges ($0\le kh\le 4.0$), and thus the number of elements was used for the ensuing further computation.

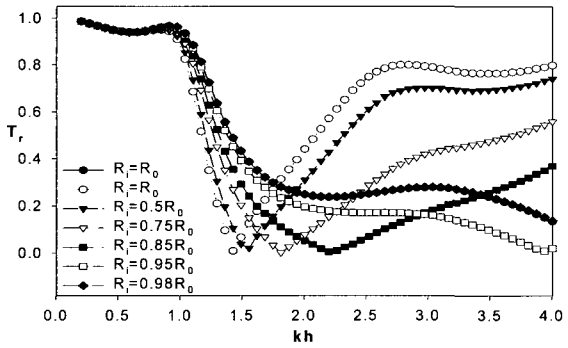

(a) transmission coefficients

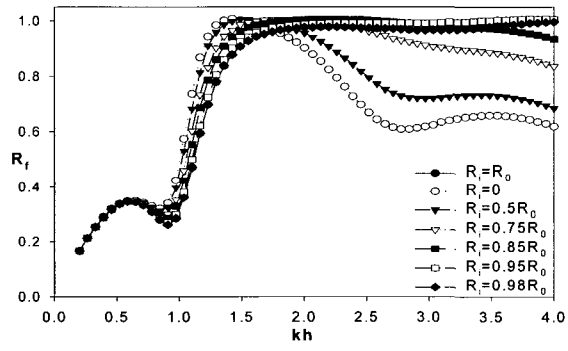

(b) reflection coefficients

Fig. 4 (a) Transmission coefficients and (b) reflection coefficients as function R_i and kh

When the large sizes of pontoons $R_0/h=0.2$ are employed to a front system with mooring type 3, and also employed to a rear system with mooring type 2. In addition, the taught mooring stiffness is employed for the both system ($T_f/k_{f1}=0.1$, $T_r/K_{r1}=0$, $T_r/K_{r2}=0.1$, $c_{ik}/h=0.125$, and $d_c/h=1$), reflection and transmission coefficients for various radius of inner pontoon are shown in Fig. 4 as function dimensionless frequency kh and wave zero heading (beam sea). The symbols R_i and R_0 in the legend of figures are represented by radius of inside and outside circular pontoon respectively. The wave blocking efficiency of half cylinder filled with water is generally poor over wide range of high frequency, when it is compared to the case of $R_i=0.85R_o$, which means 0.85 times of radius of outside circular pontoon. Although mooring type 3 and taught mooring stiffness can insure the vertical sinusoidal manner of the motion of membranes that transforms partially the incident propagating waves to the exponentially decaying local standing wave in the lee side. Such phenomena are well described in the previous study (Kee et al., 2003).

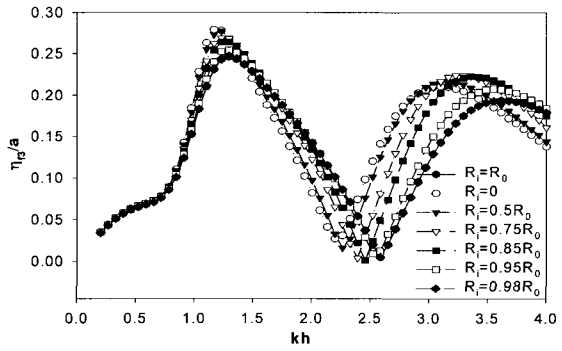

(a) sway

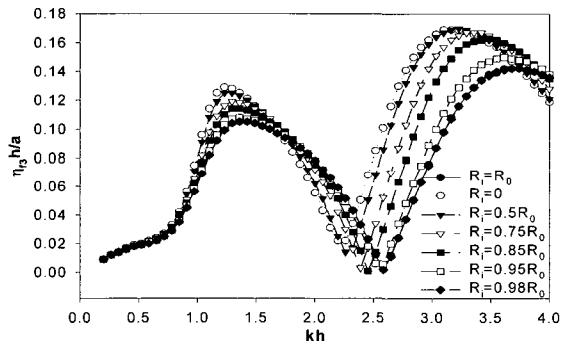

(b) roll

Fig. 5 Dimensionless motions of front double hull for R_i and kh

The hydrodynamic effects of rear pontoon with only one mooring line at joint (mooring type 2) dramatically enhanced performance of system especially due to the pivoted vibration of rear pontoon at joint. The scattered waves by the motion of rear pontoon excite mutual cancellation against incident waves or scattered waves by motion of rear membrane and front pontoon/membrane. In addition, it shows the insight of a physical phenomena magnifying the wave trapping effects between two systems.

The sway and roll motions for a front pontoon moored by type 3 are gradually reduced as radius of inside pontoon increases in the limited region of high frequency. The pattern of motions can be varied reversely in the other frequency region as shown in Fig. 5. The trends of both sway and roll motions are, however, very similar to each others.

As shown in Fig. 6, the motions of rear pontoon are larger then those of the front one, due to its pivoted vibration of joints (between pontoon and membranes) restrained by the mooring type 2. The system of half circular pontoon filled with water is much heavier than the others, thus its displacement, especially at the higher frequency regions, are much smaller, which is allowing more transmitted waves. It is mainly due to the less cancellation effects between radiated wave potential and incident wave potentials. In the lower frequency region, however, the trend is varied reversely, because of the larger exciting wave forces against lighter system with smaller net buoyancy, which are directly related to the week mooring stiffness and membrane initial tensions.

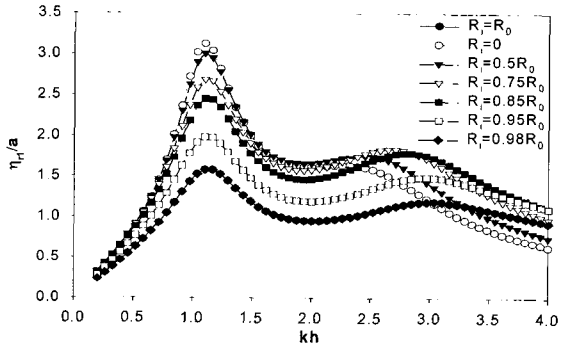

(a) sway

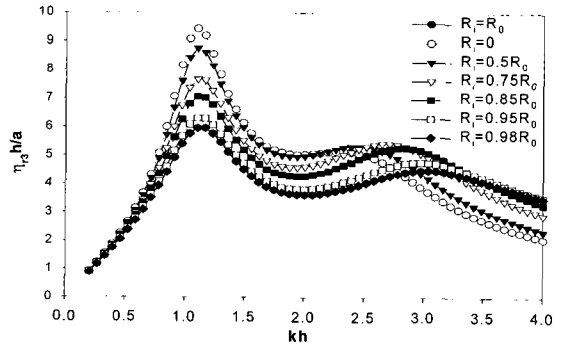

(b) roll

Fig. 6 Dimensionless motions of rear double hull for R_i and kh

There are no forces or moments exciting on the inner surface of double hull, when no inner space exist as shown in Figs. 7 and 8. It is interesting to note that the moment is gradually increased as the radius of inner circular pontoon reduces to a certain limit, for example, $R_i = 0.85R_o$ for this case, and it starts to decrease as inner radius decreases. It is mainly due to the cancellation of the excited pressures, which integrates around the geometry of inner cylindrical pontoon, from almost circular pontoon to half circular shape, through several transient and proper geometrical shapes. Thus the result confirms that the developed numerical method is valid.

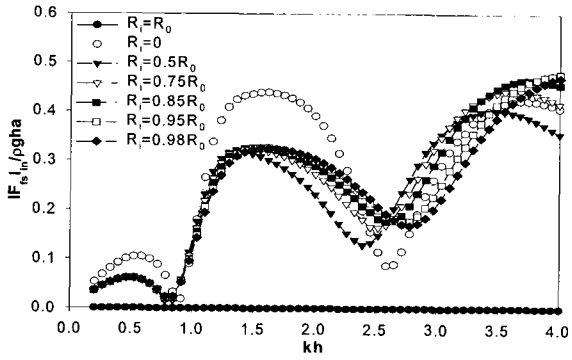

Fig. 7 Dimensionless force on inside surface of front double hull pontoon for R_i and kh

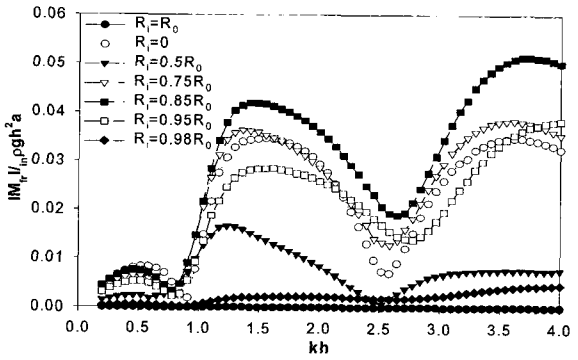

Fig. 8 Dimensionless moment on inside surface of front double hull pontoon for R_i and kh

The dimensionless forces exciting on the outer surface of exterior pontoon resemble the shape of sway motion with different order of magnitude as shown in Fig. 9 and Fig. 5a. The moments around the outer region of pontoon are the results of wave and structure interaction including the fluctuations of the inner fluid domain. The moments of $R_i = 0.85R_o$ is almost same as that of $R_i = R_o$ base on the geometrical symmetry uttered previously. Incident

wave interaction with dual submerged pontoon/membranes is quite complicated. Since it generates the radiated waves and re-reflected waves between two systems, and the radiated waves have phase differences among themselves. Adjusting these phase differences using the properly tuned parameters related with its geometry and mooring types can make their wave amplitude offset themselves. In addition, a simple large motion of membranes and pontoons does not always aggravate its performance when the generated wave by the pontoon/membrane motions and incident waves are mutually canceled in the lee side.

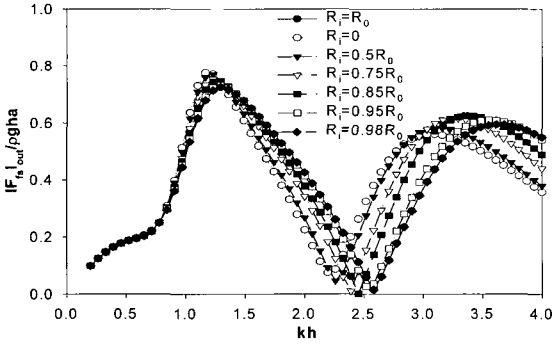

Fig. 9 Dimensionless force on outside surface of front double hull pontoon for R_i and kh

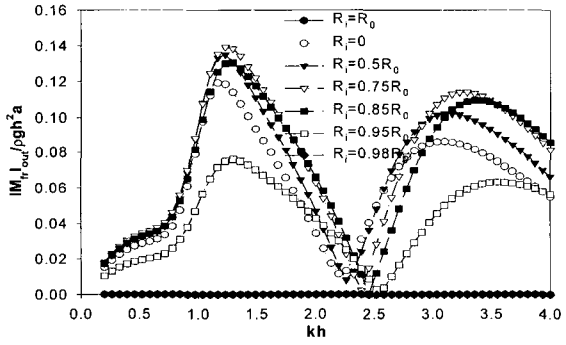

Fig. 10 Dimensionless moment on outside surface of front double hull pontoon for R_i and kh

In Figs. 11, 12, the force and moments on the whole surface of inner hull of the rear pontoon is greater than those of the front one, since the pivotal motion of pontoon is much larger than that of the front one. It is interesting to note that the force and moments on the whole surface of inner hull of the half pontoon are much suppressed, almost negligible, compared to the those of front one, due to the mutual cancelation by the radiated waves inside of the system. The forces of moments of the R_i=0.85R_o are generally large along the all frequency ranges, even though the crossroading motions of sway and roll are small.

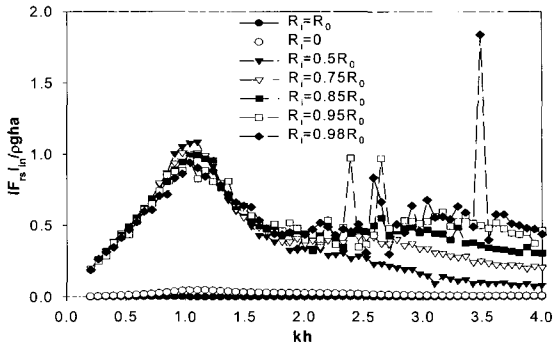

Fig. 11 Dimensionless force on inside surface of rear double hull pontoon for R_i and kh

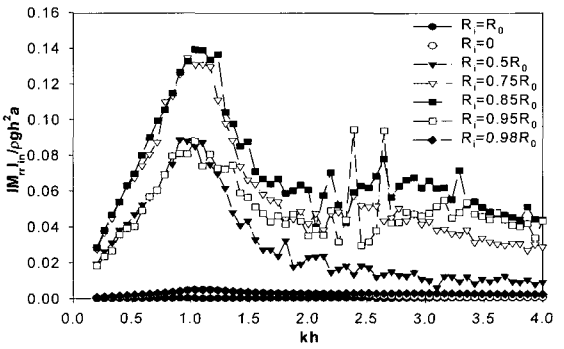

Fig. 12 Dimensionless moment on inside surface of rear double hull pontoon for R_i and kh

The frequency of the largest non-dimensional amplitudes of forces and moments on outside surface of the rear pontoon matches approximately to those of sway and roll motion as show in Figs. 13,14 and Figs. 6a,b.

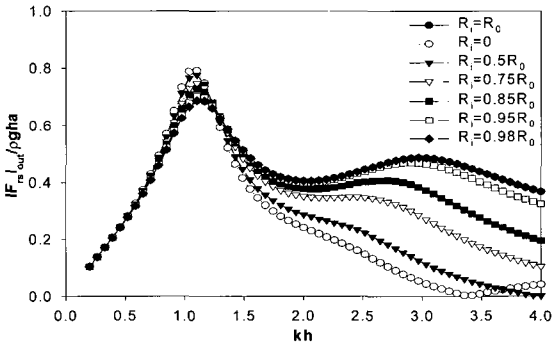

Fig. 13 Dimensionless force on outside surface of rear double hull pontoon for R_i and kh

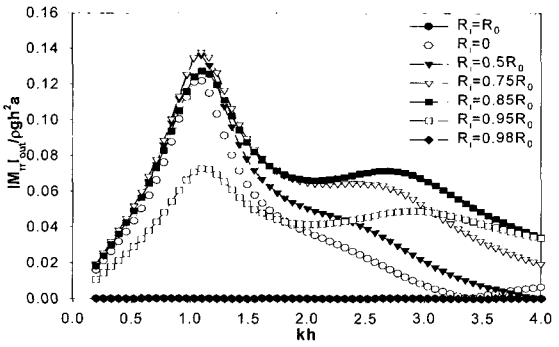

Fig. 14 Dimensionless moment on outside surface of rear double hull pontoon for R_i and kh

It is interesting to note that the roll forces on outside surface of the rear double hull pontoon are gradually increased as the radius of inner cylindrical pontoon reduces to a certain limit for example $R_i=0.85R_o$ for a case, and its starts to decrease as inner radius decreases to half circular pontoon with flat top. Thus, $R_i=0.85R_o$ is most effective radius of inner pontoon to achieve generally large moments for front or rear pontoon.

The summed forces and moments of the inner and outer regions for the front pontoon are shown in Figs. 15,16, respectively. The trends of gradually varying forces and moments as the gradual increment of the radius of inner circular pontoon are reasonable and apprehensive, as we institutively expected.

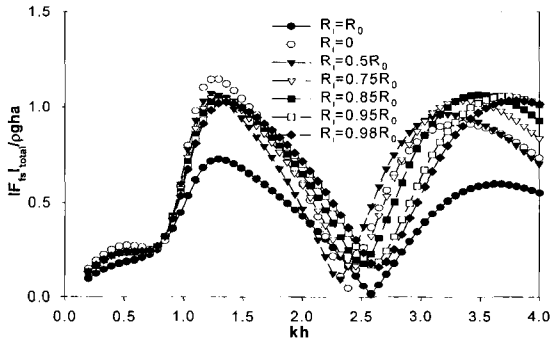

Fig. 15 Total dimensionless force on inside/outside surface of front double hull pontoon for R_i and kh

The summed forces and moments over inner and outer surfaces of the rear pontoon are, however, much lower, compared to un-summed values. Thus, we can conclude that those forces and moments are offset themselves by those phase differences. Phase differences are practical interest and shown in Figs. 17,18 for the given system, which shows the profiles that most un-scattered, un-spiked. In addition, generally small values of forces in the direction of sway are mutually canceled between inner and outer exciting forces. Thus, $R_i=0.85R_o$ is a most effective radius of inner pontoon to achieve generally small values of the total force and moments for rear pontoon.

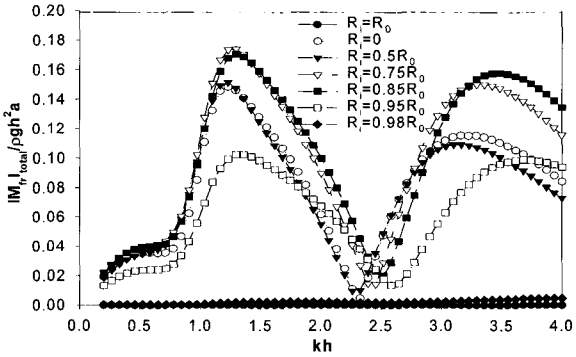

Fig. 16 Dimensionless moment on inside/outside surface of front double hull pontoon for R_i and kh

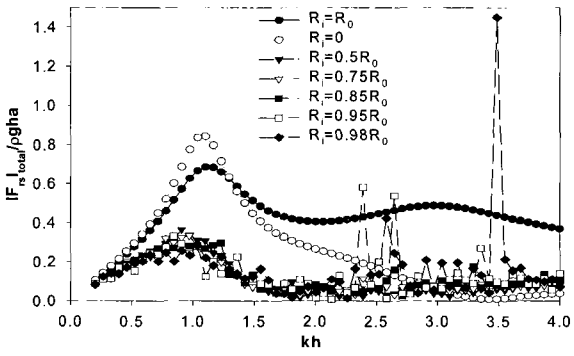

Fig. 17 Total dimensionless force on inside/outside surface of rear double hull pontoon for R_i and kh

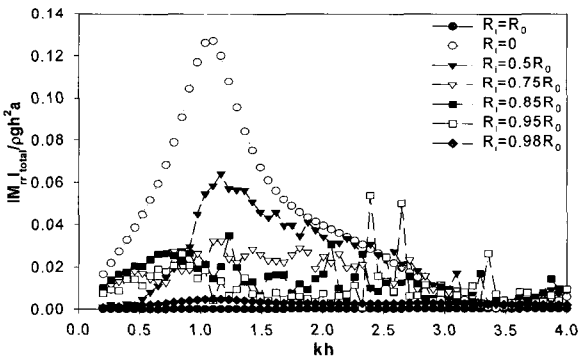

Fig. 18 Total dimensionless moment on inside/outside surface of rear double hull pontoon for R_i and kh

4. SUMMARY AND CONCLUSIONS

The interaction of incident waves with dual tensioned, inextensible, vertical flexible membranes hinged at some distance from the sea floor and attached to rigid cylindrical submerged double hull pontoons at their tops, can be solved in the context of two dimensional linear wave body interaction theory. For numerical approaches to more practical and eco-friendlier pontoon membrane systems, a boundary element program was developed based on a discrete membrane dynamic model and simple source distribution over the entire fluid boundaries. A five domain BEM was employed. Since the membrane is infinitely thin, the solutions of each domain were matched at the respective membrane surfaces. Membrane motions and velocity potentials were solved simultaneously because the body boundary condition on the membrane is not known in advance, as other hydro elastic problems. The accuracy and convergence of the developed computer program are checked using the energy conservation formula and convergence test for a limited case. Using developed program hydrodynamic characteristic of the submerged dual pontoon system with double hulls filled with water has been investigated for a beginning stage of research to the dual porous double hull pontoon/vertical porous membrane breakwater.

It is found that optimum radius of inner pontoon, i.e., optimum gap of double hull can be exist for a good performance as wave barrier compared to that of the no double hull case. Applying proper inner radius $R_i=0.85R_o$ on inner pontoon, motion of the system can be dramatically reduced to secure the safety of structural dynamics, and also guarantee reduces transmission along the mid range of frequencies. Thus we can expect intuitively, if the proper porosity is implied on outer surface of double hull, for further stage of research, the performance of breakwater can be greatly enhanced based on the wave energy dissipation through fine pores.

ACKNOWLEDGEMENT

This research was partially supported by Korea Research Foundation Grant KRF E00419.

REFERENCES

Aoki, S., Liu, H. and Sawaragi, T. (1994). "Wave Transformation and Wave Forces on Submerged Vertical Membrane", Proc. Intl. Symp. Waves Physical and Numerical Modeling, Vancouver, pp 1287-1296.

Cho, I.H., Kee, S.T. and Kim, M.H. (1997). "The Performance of Dual Flexible Membrane Wave Barrier in Oblique Incident Waves", J. of Applied Ocean Research, Vol 19, No 34, pp 171-182.

Cho, I.H., Kee, S.T. and Kim, M.H. (1998). "The Performance of Dual Flexible Membrane Wave Barrier in Oblique Sea", ASCE J. of Waterway, Port, Coastal and Ocean Engineering, Vol 124, No 1, pp 21-30.

Edmond, Y.M. (1998). "Flexible Dual Membrane Wave Barrier", ASCE J. of Waterway, Port, Coastal & Ocean Engineering, Vol 124, No 5, pp 264-271.

Lee, W.K. and Edmond, Y.M. (2002). "Flexible Dual Membrane Wave Barrier", J. of Ocean Engineering, Vol 29, No 5, pp 1782-1804.

Kee, S.T. and Kim, M.H. (1997). "Flexible Membrane Wave Barrier. Part 2. Floating/Submerged Pontoon Membrane System", ASCE J. of Waterway, Port, Coastal and Ocean Engineering, Vol 123, No 2, pp 82-90.

Kee, S.T. (2001a). "Performance of the Submerged Dual Buoy/Membrane Breakwaters in Oblique Seas", Journal of Ocean Engineering and Technology, Vol 15, No 2, pp 11-21.

Kee, S.T. (2001b). "Resonance and Response of the Submerged Dual Buoy/Porous Membrane Breakwaters in Oblique Seas", Journal of Ocean Engineering and Technology, Vol 15, No 2, pp 22-33.

Kee, S.T., Cho, I.H. and Kim, M.H. (2003). "Performance Evaluation of the Submerged Dual Buoy/Porous Membrane Breakwaters in Oblique Seas", Proceeding of The Thirteenth ISOPE, Honolulu, Hawaii, Vol 3, pp 891-899.

Kim, M.H. and Kee, S.T. (1996). "Flexible Membrane Wave Barrier. Part 1. Analytic and Numerical Solutions", ASCE J. of Waterway, Port, Coastal and Ocean Engineering, Vol 122, No 1, pp 46-53.

Thompson, G.O., Sollitt, C.K., McDougal, W.G. and Bender W.R. (1992). "Flexible Membrane Wave Barrier", ASCE Conf. Ocean V, College Station, pp 129-148.

Wang, K.H. and Ren, X. (1993). "Water Waves on Flexible and Porous Breakwaters", Journal of Engineering Mechanics, Vol 119, No 5, pp 1025-1047.

Williams, A.N. (1996). "Floating Membrane Breakwater", J. of Offshore Mechanics and Arctic Engrg., Vol 118, pp 46-51.

2005년 2월 14일 원고 접수
2005년 3월 25일 수정본 채택